

Effects of winglets to augment tube wall heat transfer in louvered fin heat exchangers

Paul A. Sanders, Karen A. Thole *

Mechanical Engineering Department, Virginia Tech, Blacksburg, VA 24060, United States

Received 27 January 2006; received in revised form 30 March 2006

Available online 14 June 2006

Abstract

The louvered fin heat exchanger, a type of compact heat exchanger, has been used heavily in the automotive and air conditioning industries for the last several decades. The majority of past research, aimed towards improving louvered fin exchanger efficiency, has focused on optimizing various parameters of the louvered fin. The experimental study presented in this paper concentrates instead on augmenting the heat transfer along the tube wall of the compact heat exchanger through the use of winglets placed on the louvers. The experiments were completed on a 20 times scaled model of an idealized louvered fin exchanger with a fin pitch to louver pitch ratio of 0.76 and a louver angle of 27°. The Reynolds numbers tested, based on louver pitch, were between 230 and 1016. A number of geometrical winglet parameters, including angle of attack, aspect ratio, direction, and shape, were all evaluated based on heat transfer augmentation, friction factor augmentation, and efficiency index (combination of both augmentations). In an attempt to optimize these winglet parameters, tube wall heat transfer augmentations as high as 39% were achieved with associated friction factor augmentations as high as 23%.
© 2006 Elsevier Ltd. All rights reserved.

Keywords: Compact heat exchangers; Louvered fin heat exchangers

1. Introduction

Louvered fins provide advantages over continuous fin designs because each louver initiates new boundary layer growth, producing higher convective heat transfer than that of a continuous fin. Fig. 1 illustrates a typical louvered fin heat exchanger geometry comprised of louvered fins and tubes. Because the thermal resistance in a typical louvered fin heat exchanger primarily results from the air side, past research has focused on increasing exchanger efficiency by designing louvered fins that maximize heat transfer. However, the tube wall is considered the primary surface where temperature differentials between the wall and convective fluid provide a high potential for heat transfer. Perturbing the flow mechanisms that could further augment the tube wall heat transfer is one means to further improve overall exchanger heat transfer.

This study experimentally explores the use of delta winglets placed on the louvers near the tube wall to augment tube wall heat transfer. Tube wall heat transfer and pressure drop measurements are reported for an idealized louvered fin geometry. Several parameters for the delta winglets were studied to give a wide range of results for determining important trends. All of the experiments were performed for a single louvered array geometry with a fin pitch to louver pitch ratio of 0.76, a louver angle of 27°, and a Reynolds number range based on louver pitch of $230 < Re < 1016$. The following sections discuss the relevant literature in this area, provide details of the experiments, and finally report the results that were acquired.

2. Past relevant studies

Much of the research related to louvered fin heat exchangers has been reported in terms of overall heat exchanger performance. There have been fewer studies focused on the detailed flow field and heat transfer

* Corresponding author. Tel.: +1 540 231 7192; fax: +1 540 231 9100.
E-mail address: thole@vt.edu (K.A. Thole).

Nomenclature

A	delta winglet aspect ratio, $A = 4(b/2)/c$	q''_{total}	applied heat flux at heated wall
b	twice winglet height	q''_{rad}	heat flux lost by radiation from the heated wall
c	winglet chord	Re	Reynolds number based on louver pitch, $Re = U_{\text{ff}}L_p/\nu$
D_H	hydraulic diameter, $D_H = \frac{4(F_p-t)F_h}{2(F_p-t)+2F_h}$	t	louver thickness
f	fanning friction factor	T_{inlet}	temperature measured at test section inlet
f_{aug}	augmentation of friction factor due to winglets, $f_{\text{aug}} = f/f_0$	T_{wall}	temperature measured on heated wall
f_0	baseline friction factor with no winglets	U_{ff}	maximum free flow velocity
F_d	fin depth, distance from leading edge of entrance louver to trailing edge of turnover louver	U_{in}	inlet velocity
F_h	fin height (distance from tube wall to tube wall)	VG-F	forwards facing delta winglet
F_p	fin pitch	VG-B	backwards facing delta winglet
k	thermal conductivity	x	streamwise coordinate through test facility
K_c	loss coefficient for sudden contraction of flow entering louvered array	X	non-dimensional fin depth, $X = x/F_d$
K_e	loss coefficient for sudden expansion of flow leaving louvered array	Z	distance of delta winglet from wall
L_p	louver pitch	<i>Greek symbols</i>	
Nu	Nusselt number, $Nu = hL_p/k$	α	winglet angle of attack
Nu_{aug}	augmentation of Nusselt number due to winglets, $Nu_{\text{aug}} = Nu/Nu_0$	θ	louver angle
Nu_0	baseline Nusselt number	η	efficiency index, $\eta = Nu_{\text{aug}}/f_{\text{aug}}$
q''_{cond}	heat flux lost by conduction through instrumented wall	ΔP	pressure drop through louvered array
		ρ_{air}	density of air
		ν	kinematic viscosity

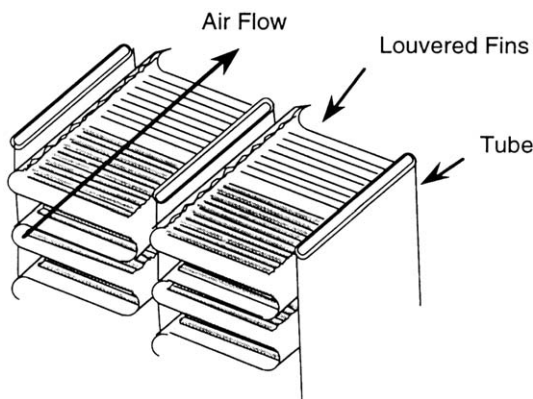


Fig. 1. Diagram of realistic louvered fin heat exchanger.

measurements within the heat exchanger, typically completed with the use of scaled-up heat exchanger models or computational fluid dynamics. There are very few studies to date that have given any detailed information of the heat transfer and flow field near the tube wall surface.

Kays and London [1] have given a compilation of heat transfer and pressure drop measurements for a large number of heat exchanger designs. Other studies of actual-sized heat exchangers, like the one performed by Achaicha and Cowell [2], provided data for a wide range of influential parameters such as fin pitch, louver pitch, tube pitch, and louver angle. Although information like this is very valu-

able, particularly from a heat exchanger design perspective, it does not offer details of the heat transfer and flow field mechanisms within the exchanger.

Studies performed with scaled-up heat exchanger models provide detailed information; however, the majority of these studies have concentrated on the two-dimensional flow region over the louvers, ignoring effects of the tube surface. For example, Webb and Trauger [3] performed flow visualization studies that showed the relationship of flow alignment with louvers for different louver angles, louver pitches, and fin pitches.

Because louvers make up the majority of the exchanger surface area, studies focused on two-dimensional effects are understandable; however, more recent studies have shown that the three-dimensional flow near the tube wall does impact the performance of the exchanger. Atkinson et al. [4] conducted two-dimensional and three-dimensional simulations for overall heat transfer and friction factor and then compared their results to experimental results of Achaicha and Cowell [2]. They reported that the ability to match computational heat transfer results to experimental heat exchanger data was much better for the three-dimensional models. They also reported that two-dimensional and three-dimensional simulations matched actual exchanger data well for friction factor, but the three-dimensional model provided better results for small tube pitches. Cui and Tafti [5] performed computational studies on a three-dimensional fin geometry. This geometry

included a louver, a transition region, and a flat landing leading to the tube wall, which are features created in the stamping process of an actual louvered fin. They showed strong three-dimensional flow field effects in the transition region caused by high energy vortex jets. These vortices were also shown to have a positive effect on tube wall heat transfer. Tafti and Cui [6] extended their 2002 study to four different louver lengths. This was a computational study detailing the heat transfer performance on the louver and tube wall surfaces as well as providing friction factors for three of these geometries. Results indicated that increasing louver length caused a decrease in tube wall heat transfer and an increase in friction factor. However, both studies [5,6] considered only a single streamwise periodic louver, ignoring the effects of the entrance, turnover, and exit louvers.

Ebeling and Thole [7] gave experimental and computational results for straight louvers with no transition at the tube wall-louver interface. These results showed that compared to a flat plate with a continuous boundary layer, the tube wall provides higher heat transfer performance resulting from the repeated interruptions on the tube wall boundary layer by the leading edges of the louvers. Their study also showed that entrance, turnover, and exit louvers provide a substantial benefit to tube wall heat transfer as the flow turns lead to significant thermal boundary layer thinning.

Although no studies have been done with vortex generators incorporated on the fins of a louvered fin heat exchanger, several have been done with them on flat plates, in channels, and in other types of heat exchangers. Gentry and Jacobi [8] performed studies with delta wings on a flat plate and in a developing channel flow, both of which were done with laminar flow. The vortex strength and heat transfer enhancements in the developing channel flow increased with increasing Reynolds number (based on hydraulic diameter), winglet aspect ratio, and angle of attack. Vortices were shown to have a significant effect on both surfaces, leading to heat transfer augmentations averaged through the entire channel of 20% and 50% at $Re_{D_H} = 400$ and 2000, respectively.

Several studies have also been completed with delta winglets placed in finned oval tube heat exchangers. These types of exchangers lend themselves to enhancement with vortex generation due to the large plate areas from which winglets can be stamped. Chen et al. [9] performed a computational study where three different configurations of inline punched delta winglets were placed on either side of the tube. Their study showed that the longitudinal vortex from the upstream winglet merges with the vortex from the downstream winglets to form a larger, stronger vortex that provides higher heat transfer than a single winglet. When a third winglet was added in line, the same trends occurred. These studies also showed that each successive winglet increases the pressure drop through the exchanger. A similar computational study by Tiwari et al. [10] had configurations with one, two, three, and four inline pairs

of non-punched delta winglets in a flat plate oval tube exchanger. Their results also showed an increase in heat transfer with increasing number of inline winglets. They showed results for winglets that were staggered and alternating in direction, which produced higher heat transfer augmentations than the in-line winglets in the same direction. Although these and other similar studies in tube plate heat exchangers have winglets applied to the fin surface in the near tube region, it seems that no research has been done where winglets have been placed near enough to the tube wall to try and augment tube wall heat transfer.

Joardar and Jacobi [11] seem to be the only researchers who have combined delta wings and louvered fin heat exchangers. In their study, delta wings were glued to the tubes at the leading edge of the fins in an actual louvered fin heat exchanger. The exchanger was tested in dry and wet conditions and overall heat transfer and friction factor measurements were made. Heat transfer augmentations of 21% and 23% were shown for dry and wet conditions, respectively, with an associated pressure drop penalty of 6%.

Although these studies have shown gains on the fin surface, none have been aimed at increasing tube wall heat transfer. The single study with longitudinal vortices in louvered fin heat exchangers did not incorporate winglets into the exchanger itself, but applied wings to the outside of the exchanger. The work presented in this paper is aimed at augmenting the heat transfer along the tube wall through the use of delta winglets.

3. Experimental facility and instrumentation

All tests were carried out in a 20 times scaled version of a louvered fin exchanger. Fig. 2 shows the test facility used in this study, which was an open loop wind tunnel consisting of an inlet nozzle, a test section, a laminar flow element, and a motor-controlled blower. All of the major components in the test facility were the same used in the studies of Lyman et al. [12], Stephan and Thole [13], and Ebeling and Thole [7], with the exception of the test section. The contraction was designed to provide a uniform inlet flow to the test section, which had a nozzle with a 16:1 area

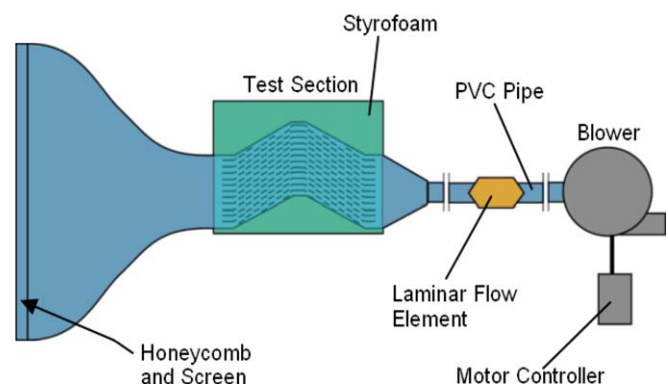


Fig. 2. Test facility used for tube wall studies with winglets on louvers.

reduction. Flow rates through the test section were measured by a laminar flow element. Air was pulled through the test rig with a 1.5 hp motor powering a centrifugal fan, which was controlled with an AC inverter.

The test section was composed of the bounded flow path through the louvered fin array, an instrumented heated wall, and a conduction guard heater assembly. The top and bottom walls bounding the flow path replicated the louver angles to simulate louver directed flow. The louvered test section had 12 louver rows, which was based on studies by Springer and Thole [14] that showed 12 rows were adequate to model an infinite stack of louvers. The louver geometry used for all testing was $\theta = 27^\circ$, $F_p/L_p = 0.76$, and $t = 0.079L_p$ (see Fig. 3). This array was composed of an entrance louver, seven streamwise louvers, a turnover louver, seven additional streamwise louvers, and finally an exit louver. Note that for this study, the louvers were idealized as continuous across the fin height with no modeling of the transition region between the tube wall and the fin itself.

The instrumented heated wall, which provided a constant heat flux boundary condition, simulated the tube wall in an actual heat exchanger. It was constructed from 20 equally sized strip heaters arranged in series that were adhered to a sheet of lexan. The entire heater spanned from the beginning of the entrance louver to the end of the exit louver and from the bottom wall to the top wall. Current through the heater circuit was measured by a precision resistor that was connected in series with the heater. This current, along with the heater resistance and surface area, were used to calculate the heat flux. Thermocouples were embedded in the lexan, directly behind the heater, so that streamwise temperature measurements could be made.

Because the intent of this study was to make tube wall heat transfer measurements, it was important to isolate and quantify losses from the heated wall to the louvers and through the back side of the heated wall. To minimize the conduction losses through the back side of the heated wall, low thermal conductivity foam was placed directly behind it. On the outside of this foam was a guard heater, which was composed of an aluminum sheet with thermocouples bonded to one side and a heater on the other side. The heater was used to minimize conduction losses by

matching the temperatures across the foam. On the back side of this assembly was more insulation to further reduce conduction losses. Using these guard heaters, typically only 0.5–4.0% of the applied heat flux to the heated wall was lost through conduction.

Steps were also taken to minimize conduction and radiation losses from the heated wall to the louvers. The louvers were made from balsa wood which had a low enough thermal conductivity to simulate nearly adiabatic fins. Silver paint ($\epsilon = 0.3$) was used on the louvers to minimize radiation losses from the wall to the louver surfaces. The fins were attached to the heated wall by using small brackets that were adhered with double-sided tape to the wall in the array geometry. The other end of the louver was held in place by a milled wall, with slots matching the array geometry.

Temperature measurements were made with type E thermocouples placed behind the strip heaters. The thermocouple arrangement consisted of 20 center channel thermocouples and 20 thermocouples to verify periodicity in the adjacent louver channels. While temperature measurements will only be given for the center channel thermocouples, periodicity in the pitch direction indicated no more than a 5% difference between louver channels. Once the tunnel was at steady state, an average of 200 temperature measurements was taken at each thermocouple location.

Pressure drop measurements across the louvered array were made with a 0–0.1 in H₂O pressure transducer connected to a pressure tap $0.73L_p$ upstream of the entrance louver and one $0.73L_p$ downstream of the exit louver. To obtain pressure drop measurements through the louvered array and the laminar flow element, 1500 and 500 samples, respectively, were taken and averaged. Typically 200 samples were averaged to obtain the louvered array pressure drop at each Reynolds number. Reynolds numbers for the pressure drop measurements were always matched to within $Re = \pm 0.5$ of the target Reynolds number before data was collected. To obtain physically realistic winglet pressure drop results, two winglets were placed on each louver (one by each wall).

As previously stated, the conduction losses were minimized through the use of the guard heater, but were still

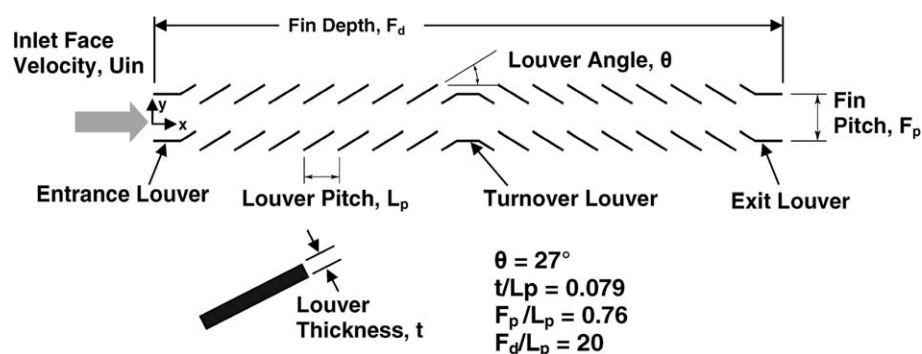


Fig. 3. Louvered array geometry and definitions used in this study.

accounted for in the data reduction. The losses due to radiation from the heater were accounted for through the use of view factor equations given by Modest [15]. Local Nusselt numbers were then calculated using the following relation:

$$Nu = \frac{q''_{\text{total}} - q''_{\text{cond}}(X) - q_{\text{rad}}(X)}{T_{\text{wall}}(X) - T_{\text{inlet}}} \frac{L_p}{k_{\text{air}}} \quad (1)$$

Nusselt number and friction factor augmentations were simply calculated as the ratio of winglet test values to baseline values (no winglets). Heat transfer results for the entrance louver thermocouples were not accounted for in the area-averaged augmentation values seen in this paper because no winglets were ever placed on the entrance louver. Likewise, winglets were not placed on the turnover and exit louvers; however, heat transfer values at these locations were accounted for in augmentation calculations because they were affected by upstream winglets.

The pressure drop measurements through the array were converted to Fanning friction factors with the following equation,

$$f = \frac{D_H}{4F_d} \left(\frac{2\Delta P}{U_{\text{ff}}^2 \rho_{\text{air}}} - K_c - K_e \right) \quad (2)$$

where K_c and K_e are loss coefficients of the sudden contraction and expansion associated with the air entering and leaving the finned array. Both coefficients were found to be 0.03 by using a duct area reduction and expansion chart [16].

The uncertainty estimates of Nusselt numbers, Reynolds numbers, and friction factors were calculated using the method described by Moffat [17] which is based on the chain rule of differentiation. Uncertainties in Nusselt numbers for the majority of the louvered array were 4.4% at $Re = 230$ and were 2.8% at $Re = 1016$. Higher values occurred at the first louver position, but as stated above, these values were not used in augmentation calculations. Uncertainties in the baseline friction factor for $Re = 230$ were a high 51%, due to the very low pressure differences, and were 8.2% at $Re = 1016$.

4. Baseline heat transfer and pressure drop results

From a flow standpoint, the test facility used in this study was the same as that used by Lyman et al. [12], so benchmarking related to inlet flow uniformity and number of louvers necessary to assume an infinite stack of louvers was not repeated. The benchmarking associated with heat transfer measurements involved confirming periodicity in the pitch and making comparisons to results previously shown by Ebeling and Thole [7]. Friction factor results were compared to data from actual heat exchanger experiments as taken by a manufacturer.

Comparisons of the baseline results with no winglets were made to Ebeling and Thole [7] for all three Reynolds numbers. These results as a function of non-dimensional fin-depth, $X = x/F_d$, can be seen in Fig. 4. The absolute rel-

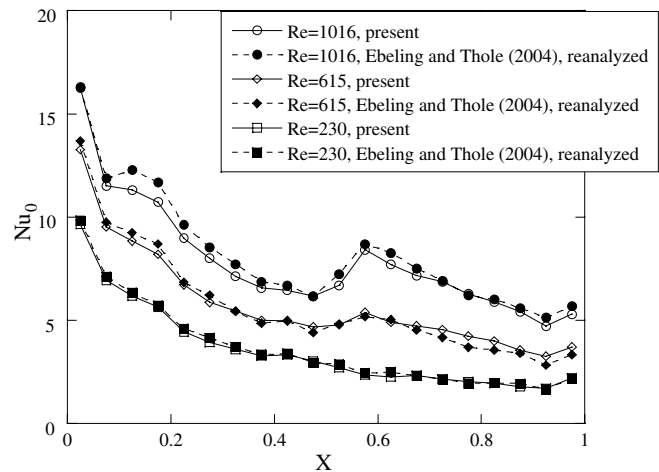


Fig. 4. Comparison of present to Ebeling and Thole's [7] baseline heat transfer results at $Re = 1016, 615, 230$.

ative percent differences between the present results and Ebeling and Thole's [7] results were 4.6%, 5.6%, and 2.9% for $Re = 1016, 615,$ and 230 , respectively. It can also be seen from these baseline results that there are some differing trends between the $Re = 230$ relative to the 1016 case. For the $Re = 1016$ case, it is clear that the tube wall heat transfer is affected by the turnover louver as illustrated by the sharp changes in slope at the entrance and at $X = 0.6$. For $Re = 230$, the tube wall Nusselt numbers continuously decrease as flow progresses along the tube wall. This effect is produced by low fluid momentum at $Re = 230$ causing the flow to respond weakly to the directional changes in the turnover louver. The dependence of the ability to turn flow on Re has significant implications on winglet performance at $Re = 230$, as will be seen in following sections.

Baseline friction factor results with no winglets can be seen in Fig. 5 compared to data from an actual heat exchanger manufacturer for nearly the same geometry. The data indicate a slightly higher friction factor which is primarily due to the modeling of the louver as straight with no transition to the tube wall. Tafti and Cui [6] showed that straight louvers produce higher friction factors than do louvers with a transition to the tube wall as a result of the increased form drag near the tube surface.

5. Winglet geometries and experimental design

The goal of this study was to find a realistic method to augment the heat transfer along the tube wall. After several options were explored, delta winglets were chosen as a promising means to accomplish this goal while minimizing the increase in overall pressure drop. Delta winglets, not to be confused with delta wings, are triangular shaped protrusions that can be placed on or stamped from a surface. Benefits are achieved from longitudinal vortices off of the trailing edge promoting bulk fluid mixing and therefore higher heat transfer. Fig. 6 shows a schematic of such a

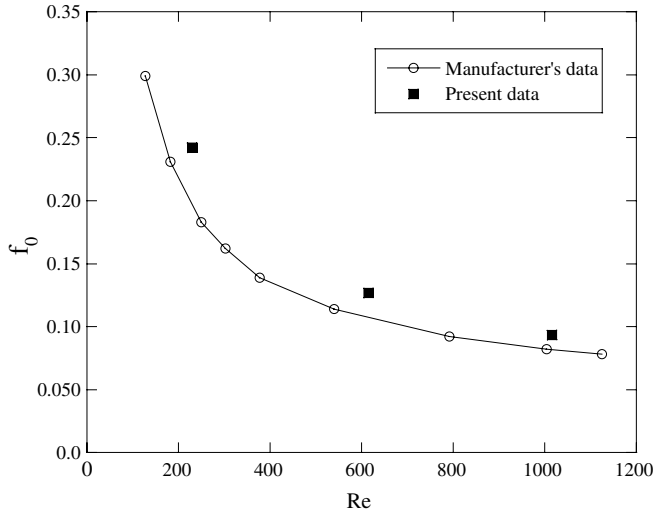


Fig. 5. Comparison of friction factor results from this study to a manufacturer's measured data.

winglet placed on a louver as well as definitions of delta winglet geometry. Note that during experiments symmetric conditions were maintained by placing winglets on both tube wall sides for each louver. A delta winglet has primarily three different parameters that geometrically describe it: aspect ratio (A), angle of attack (α), and winglet thickness. As seen in Fig. 6, A is based on the relative side lengths of the delta winglet and is defined as $A = 4(b/2)/c$. α is the angle of the winglet with respect to the incoming flow direction. In this study, all of the winglets had equal heights ($b/2$) of $0.27L_p$ whereby the winglet length (c) was altered

to vary A . Values of A used in this study were 1.5, 2, and 3, where $A = 1.5$ is the largest winglet. The chosen values for α were 20° , 30° , and 40° . The final single winglet parameter, thickness, was kept constant at $0.03t$, where t is the thickness of the louver. Along with the parameters that define the geometry of a single winglet, there are three parameters that describe the geometry with relation to the tube wall surface near which the winglets are applied. Finally, when several winglets are applied in a system, there are parameters that describe the overall system geometry.

In this study, winglets were affixed to the louver surfaces but heat transfer benefits to the tube wall were being measured. Therefore, the parameter distance from wall (Z), was defined as the distance from the tube wall to the nearest part of the winglet. Fig. 6 shows this as the downstream portion of the winglet, but it could also be the upstream portion if the winglet were placed in a different angle of attack. Values of Z tested in this study were $0.15L_p$, $0.22L_p$, and $0.29L_p$. The differences in these values are very small, but it was believed that improved performance would be achieved with the winglets closer to the wall.

Along with the distance from the wall, the proximity of the winglets to the tube wall also made winglet direction and orientation important factors. Winglet direction in this paper is defined as whether the downstream portion of the winglet is directed toward or away from the tube wall, and will be denoted in the text as "toward" and "away". Orientation is defined as to which portion of the winglet is facing upstream (see Fig. 6). In typical delta winglet studies, winglets are aimed so that the thin end of the winglet is upstream, relative to the flow, while the thicker end is

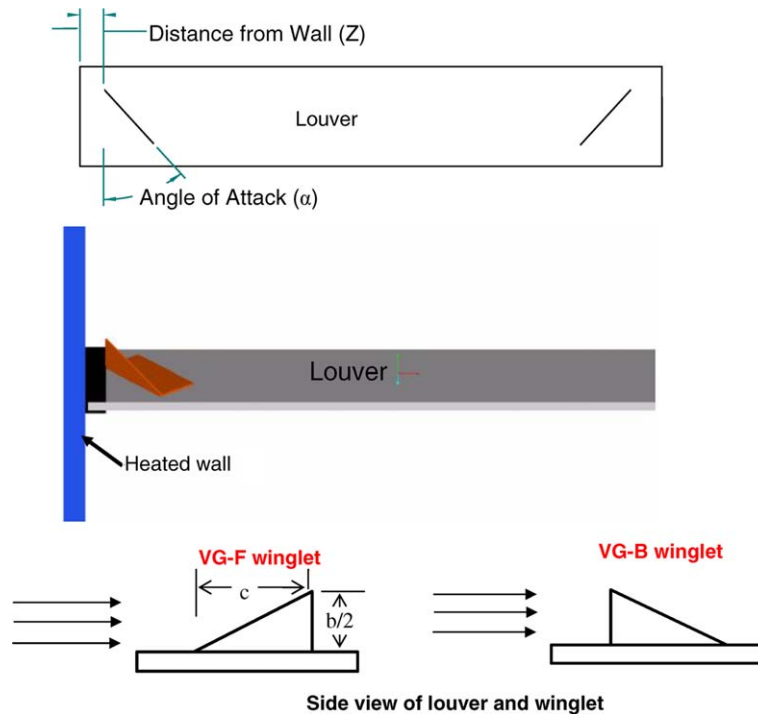


Fig. 6. Definition various winglet parameters.

downstream. In this paper, this will be described as a forward vortex generator, or VG-F. At the beginning of this study, only the VG-F orientation was tested. In an attempt to find the maximum heat transfer augmentations, winglets with the opposite orientation were also tested. This orientation will be called backward vortex generator, or VG-B.

Like direction and orientation, the overall setup of the system of winglet also proved to have a significant effect on the tube wall heat transfer and exchanger pressure drop. This is consistent with studies like those by Chen et al. [9] and Tiwari et al. [10] who showed that placing winglets in-line, staggering them, or alternating their direction did have an effect on heat transfer results. In this study, three primary winglet setups were tested and can be seen in Figs. 7a–c. As stated in the previous paragraph, initial tests were performed with winglets aimed toward the wall in the VG-F orientation (see Fig. 7a). Further testing was completed with winglets of alternating direction and orientation, as seen in Fig. 7b. The configuration in 7b is referred to VG-F/B. Also, there were several tests conducted with winglets only in the VG-B orientation but alternating in direction, as seen in Fig. 7c. Note that all experiments were completed with winglets on the bottom surface of all lou-

vers downstream of the turnover louver. Results indicated (not shown in this paper) that downstream of the turnover louver, fluid contact with the louvers and winglets was greater on the bottom surface, producing higher heat transfer augmentations (Figs. 7a–c).

Along with all of the delta winglet parameters mentioned above, a few tests were conducted with rectangular winglets. This served as a good comparator of shape and surface area to the delta winglets results.

Because of the numerous parameters that defined winglet shape and placement on the louver surfaces, steps were taken to reduce the overall number of tests. Test matrices included three categories of testing: tests derived from a design of experiments (DOE) to obtain parameter importance levels and an optimization; tests to confirm or deny the optimization found from the DOE; and tests varying parameters not studied in the DOE.

The Taguchi method [18] was chosen for deriving the design of experiments. There were four parameters studied (α , Z , A , and Re) and three levels of each parameter. This combination of parameters and levels fit into a Taguchi L-9 array, which only required that nine tests be completed to obtain trend information and an optimized parameter set.

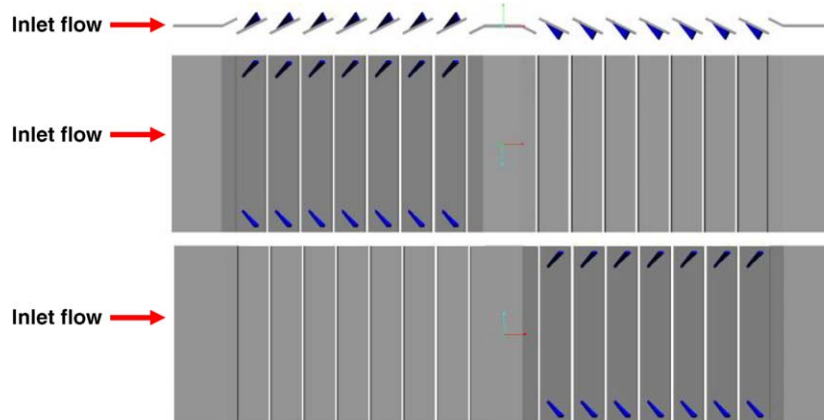


Fig. 7a. Side, top, and bottom view of VG-F winglets all aimed towards the wall.

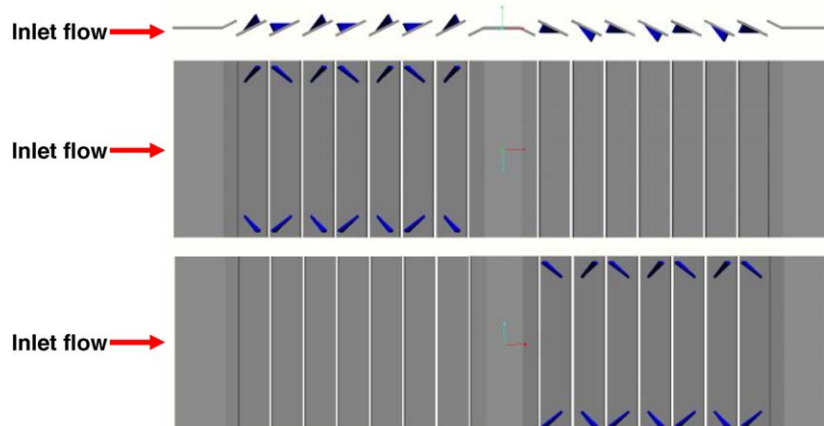


Fig. 7b. Side, top, and bottom view of VG-F/B alternating winglets.

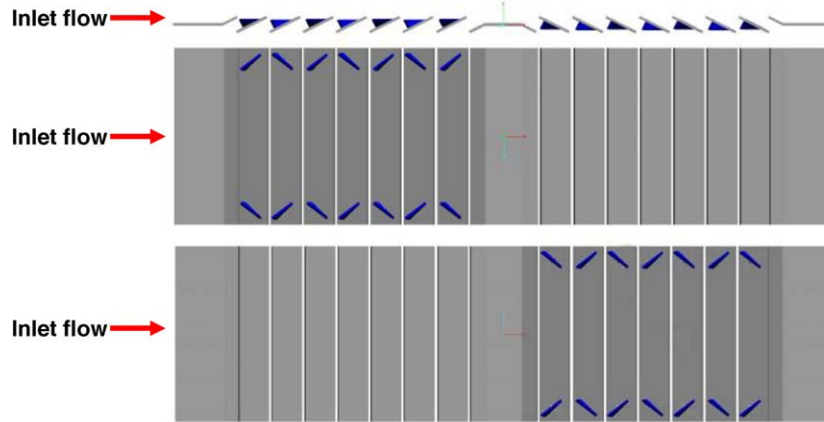


Fig. 7c. Side, top, and bottom view of VG-B winglets with alternating direction.

6. Results from design of experiments test matrix

Preliminary tests indicated that winglets aimed toward the wall in the VG-F orientation, as shown in Fig. 7a, produced very small increases in tube wall heat transfer (less than 4%). Additional tests with alternating winglet direction and orientation, as shown in Fig. 7b, indicated that there was a significant augmentation to the resulting tube wall heat transfer. As can be seen by Fig. 7b, the winglet direction and orientation (VG-F/B) were altered on every other louver in an attempt to create a circulation of the air to and from the wall relative to the center channel. For the DOE test matrix only the alternating winglets, shown in Fig. 7b, were used.

The area-averaged tube wall augmentation values for the DOE test matrix are given in Table 1. The results in Table 1 indicate that heat transfer augmentations as high as 20% could be achieved over the baseline using the winglet configuration in 7b. Also indicated by these tests, there were a number of instances that occurred with either little or negative (indicating less heat transfer than the baseline) heat transfer augmentations.

Using the results in Table 1, the relative importance of the various winglet parameters was found through further analysis of the data. The overriding influential parameter to Nusselt number augmentation was the Reynolds number. At $Re = 230$, no augmentation benefit was achieved while results at $Re = 615$ and 1016 had higher and or nearly equal

augmentations. Although this information is useful, Reynolds number could not be set to an optimum value in an application like a car radiator, but set rather by driving speed. Of the geometrical winglet parameters, angle of attack was the most influential, followed closely by aspect ratio. Heat transfer augmentation was not sensitive to variations in the distance of the winglet from the wall, possibly because chosen values were so close to each other. However, the highest heat transfer was achieved with $Z = 0.22L_p$ followed by $Z = 0.15L_p$ and $0.29L_p$. Concerning angle of attack, there was no augmentation benefit with winglets at $\alpha = 20^\circ$, while results for $\alpha = 30^\circ$ and 40° were promising. The DOE results showed that nearly equal heat transfer augmentations were possible with $\alpha = 30^\circ$ and 40° with slightly better results for $\alpha = 30^\circ$. Regarding the aspect ratio, the data indicated a decrease in augmentation with increasing A . Like $Re = 230$ and $\alpha = 20^\circ$, $A = 3$ also showed no benefit to heat transfer augmentation. To briefly summarize, the DOE results found the optimum condition for the configuration in Fig. 7b to be $Re = 1016$, $\alpha = 30^\circ$, $A = 1.5$ and $Z = 0.22L_p$. Poor heat transfer augmentation results were obtained for any experiments with $Re = 230$, $\alpha = 20^\circ$, or $A = 3$.

The DOE results provided an optimized parameter set, but several parameter levels performed nearly equally. Tests were completed in which these high performers were directly compared, to determine if a clear optimization could truly be found. $Re = 1016$ was compared to $Re = 615$, $\alpha = 30^\circ$ to $\alpha = 40^\circ$, and $Z = 0.22L_p$ to $Z = 0.15L_p$. Heat transfer results for these tests can be seen in Figs. 8–10. Next to the legend in each plot are the area-averaged percent augmentations for each of the trials. Fig. 8 shows the comparison of distance of the winglet from the wall in terms of stream wise Nusselt number. There is not much separation in the results, yielding only a 2.8% difference in area-averaged augmentation. Fig. 9 shows the comparison of angle of attack, in which results for $\alpha = 30^\circ$ and 40° have less than 0.5% difference in average augmentation.

Results for the Reynolds number comparison are given in Fig. 10 in terms of augmentation at each stream wise

Table 1
Results from DOE matrix with alternating winglets

Re	α ($^\circ$)	Z	A	Nu_{aug} (%)
230	20	$0.15L_p$	1.5	-5.65
625	30	$0.15L_p$	2	15.90
1016	40	$0.15L_p$	3	9.71
1016	20	$0.22L_p$	2	6.47
230	30	$0.22L_p$	3	-4.54
625	40	$0.22L_p$	1.5	20.04
625	20	$0.29L_p$	3	-0.11
1016	30	$0.29L_p$	1.5	19.81
230	40	$0.29L_p$	2	-2.17

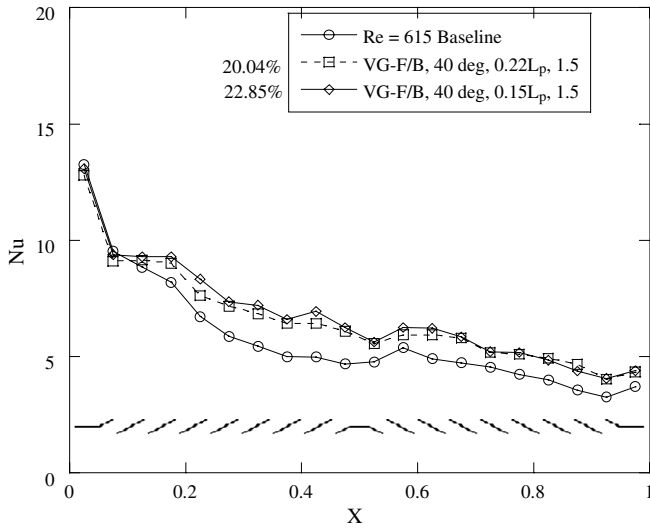


Fig. 8. Comparison of $Z = 0.15L_p$ and $0.22L_p$ with alternating winglet orientation and direction, $\alpha = 40^\circ$, $A = 1.5$, and $Re = 615$.

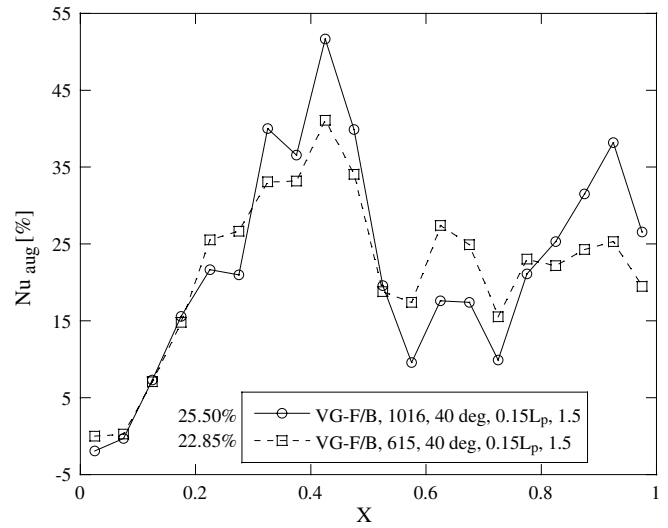


Fig. 10. Comparison of $Re = 615$ and 1016 with alternating winglet orientation and direction, $\alpha = 40^\circ$, and $A = 1.5$, $Z = 0.15L_p$.

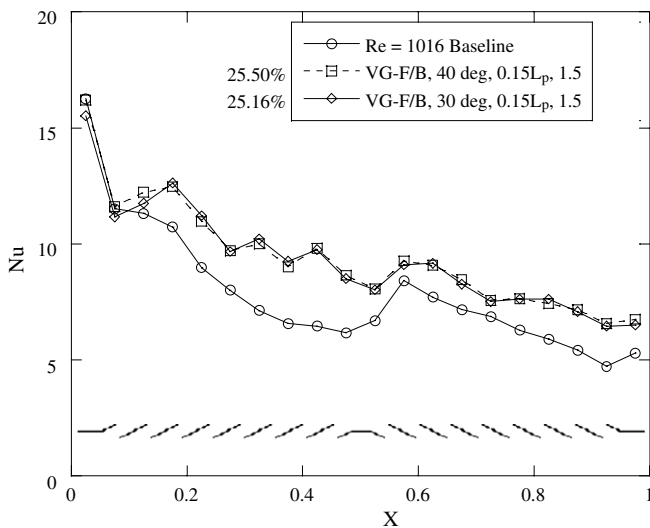


Fig. 9. Comparison of $\alpha = 30^\circ$ and 40° with alternating winglet orientation and direction, $Z = 0.15L_p$, $A = 1.5$, and $Re = 1016$.

position. The average augmentation for $Re = 1016$ was only 2.6% higher than that of $Re = 615$. Also looking at Fig. 10, it is interesting to note that the highest augmentations were found at $X = 0.425$, which is one louver position upstream of the turnover louver. In all tests with reasonable heat transfer augmentation, the maximum augmentation occurred at this location. After completing the direct comparison trials, a different optimization for the winglets in 7b was found than that given from the DOE approach. However, because differences in average augmentations between the two highest performers for Re , α , and A were all less 3%, no strong generalizations, other than good augmentations can be achieved, were made about an optimized parameter set.

7. Comparisons of winglet orientations

The results given in the previous section were all for the configuration in Fig. 7b, in which winglets alternated in direction and orientation. Further tests were conducted in which VG-F winglets were compared to VG-B winglets, so that the effect of winglet orientation could be isolated. The results of such a test can be seen in Fig. 11. In this figure, the squares represent a case with alternating winglet direction and orientation. The diamonds represent a case with VG-F winglets upstream of the turnover louver and VG-B winglets downstream of the turnover louver. Notice that upstream of the turnover louver, the VG-F winglets did not perform as well as the alternating VG-F/B winglets.

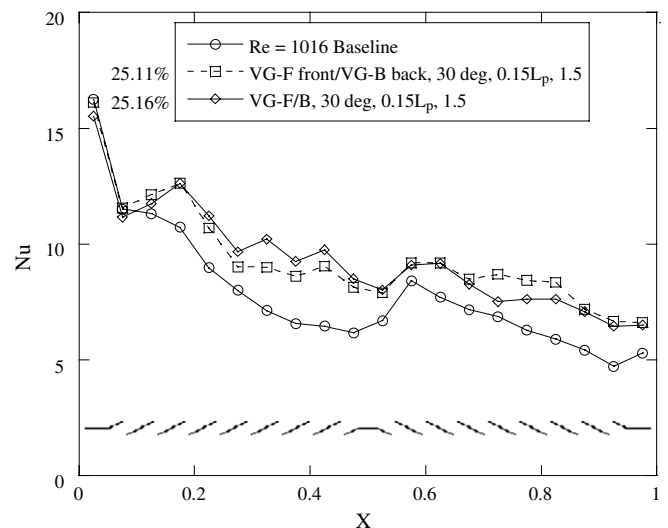


Fig. 11. Comparison of winglet orientation, with winglets upstream of the turnover in VG-F orientation and winglets downstream of the turnover in VG-B orientation. Winglet direction is alternating and $\alpha = 30^\circ$, $A = 1.5$, $Z = 0.15L_p$, and $Re = 1016$ for both cases.

The opposite occurred downstream of the turnover where VG-B winglets showed higher than or equal augmentations to the VG-F/B case. Tests like this one proved that with alternating winglelet direction, backwards winglelets (VG-B) yielded higher heat transfer augmentations than forwards (VG-F) winglelets. This led to a set of experiments with only VG-B winglelets alternating in direction (Fig. 7c). Fig. 12 shows a case with VG-B winglelets compared to the alternating VG-F/B winglelets. Notice that downstream of $X = 0.175$, the VG-B winglelets produce higher Nusselt numbers than do the alternating VG-F/B winglelets, producing an increase in average augmentation of about 9%.

Through initial experimentation, it was shown that winglelets that alternated in direction produced higher heat transfer augmentations than winglelets aimed toward the wall. It was also shown that when the winglelets were alternating in direction, the backwards (VG-B) orientation performed better than the forward (VG-F) orientation. To further test the effect of winglelet shape, rectangular winglelets (RW) were tested. Several experiments were conducted for both VG-B winglelets and rectangular winglelets (RW) at some of the better performing parameter levels so direct comparisons between winglelet shape and parameter levels could be made. For the results given in this paper, the RW were the same length (c) and height ($b/2$) as the VG-B and VG-F winglelets, which results in twice the surface area. The area-averaged augmentation values for the heat transfer results are seen in Fig. 13. At $Re = 230$, all of the results show nearly zero augmentation. As mentioned earlier in the paper, low fluid momentum at $Re = 230$ does not lend itself to augmentation from directional changes. These low augmentation values were measured for all winglelet geometries tested at $Re = 230$, including results not given here. At $Re = 615$, all three of the RW cases tested were above 35% augmentation, while only the VG-B winglelets at $\alpha = 40^\circ$ were as high. Both of the $\alpha = 30^\circ$

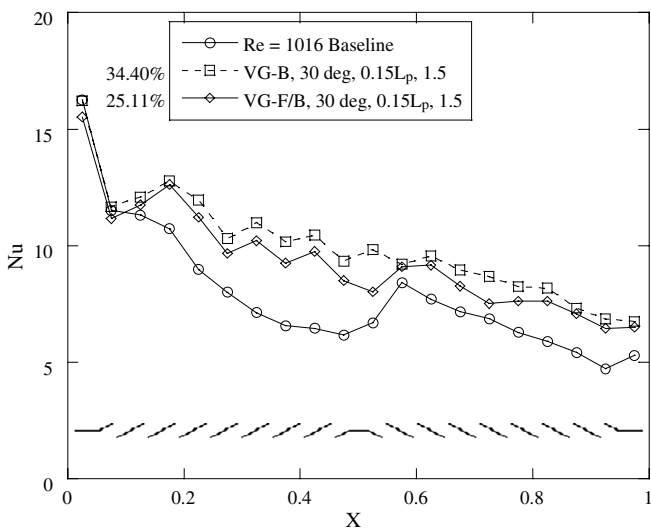


Fig. 12. Comparison of winglelet orientation with all winglets in VG-B orientation with alternating direction. $\alpha = 30^\circ$, $A = 1.5$, $Z = 0.15L_p$, and $Re = 1016$ for both cases.

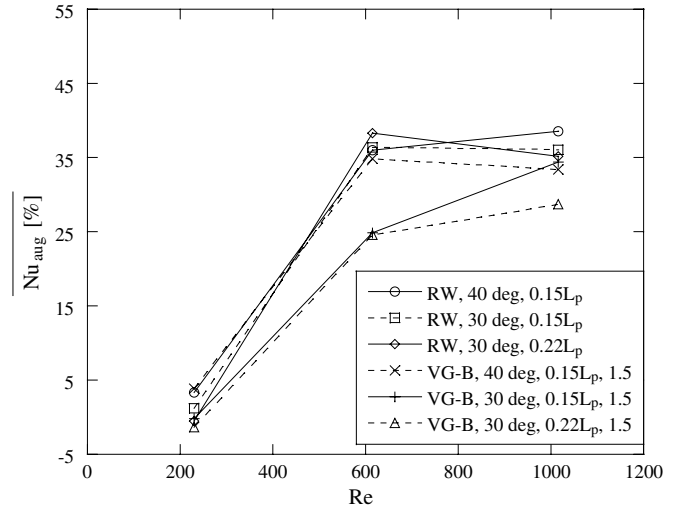


Fig. 13. Heat transfer augmentation comparisons for winglelet shape, α , and Z at all Re .

VG-B winglets produced augmentations of about 25%. At $Re = 1016$, the highest heat transfer performer was the RW at 40° and $Z = 0.15L_p$. All other results, with the exception of the VG-B winglets at $\alpha = 30^\circ$ and $Z = 0.22L_p$ showed similar heat transfer augmentations in the mid 30% range.

From the summary of data in Fig. 13, several conclusions can be made about winglelet shape, α , Z , and Re . First, no matter how high the augmentations are for $Re > 230$, the results for $Re = 230$ show little to no augmentation. At higher Reynolds numbers, rectangular winglelets (RWs) showed better augmentation than the VG-B winglets. Regarding distance from the wall, the results indicated that closer is better with $Z = 0.15L_p$ producing higher augmentations than $Z = 0.22L_p$. The angle of attack comparisons indicated that $\alpha = 40^\circ$ winglets yielded higher heat transfer than the 30° winglets for VG-B winglets, and the results for the rectangular winglets showed little differences between the two angles of attack. There were also conflicting results for which Reynolds number produced the highest heat transfer augmentation. Three of the tests showed increased augmentation levels from $Re = 615$ to $Re = 1016$ while the other three showed decreased augmentation levels. Averaged over all three Reynolds numbers, the best overall heat transfer performer was the RW at $\alpha = 40^\circ$ and $Z = 0.15L_p$.

8. Pressure drop and efficiency index results

The previous sections described the differences in heat transfer augmentations caused by changes in winglelet geometrical parameters and Re . It is also important to evaluate the winglets in terms of increase on heat exchanger pressure loss. In this study, channel pressure loss measurements have been converted to Fanning friction factors. Friction factor augmentation results are given in Fig. 14, which correspond to the same geometries for the heat transfer augmentations given in Fig. 13. As expected, several of

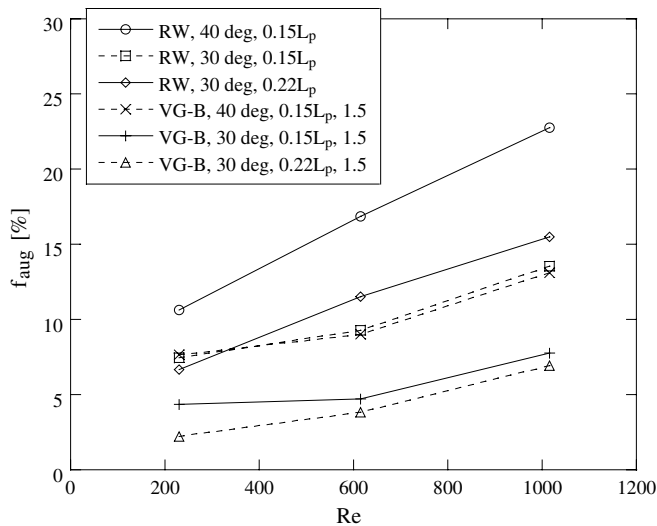


Fig. 14. Friction factor augmentation comparisons for winglet shape, α , and Z at all Re .

the trends for heat transfer augmentations are also seen in the friction factor augmentations. The rectangular winglets yielded higher friction factor augmentations than the VG-B winglets, due to the increased surface area. Moreover, winglets with $\alpha = 40^\circ$ produced higher friction factor augmentations than 30° winglets, also caused by the increased blockage to the flow. Regarding the distance from the wall, $0.15L_p$ showed lower friction factor augmentation for rectangular winglets and higher for VG-B winglets. For all cases, friction factor augmentation increased with increasing Re .

The winglet case having the minimum friction factor augmentation was VG-B winglets at 30° and $Z = 0.22L_p$, which indicated only a 7% augmentation at $Re = 1016$. This augmentation value may seem low, but not when considering the small portion of the louver that the winglet occupies.

One way in which we can compare the relative increase in heat transfer augmentation to friction factor augmentation, is to evaluate the ratio of each. This ratio will be referred to as the efficiency index, η . The efficiency indices for the heat transfer and friction factor augmentations given in Figs. 13 and 14 can be seen in Fig. 15. On average, the VG-B winglets outperformed the RW with the only exception being the 40° VG-B winglets, which were less efficient than the rectangular winglets at $\alpha = 30^\circ$ and $Z = 0.15L_p$. Fig. 15 indicates that all cases produced nearly zero efficiency at $Re = 230$, due to the very small heat transfer augmentation results that make up the numerator in the calculation. $Re = 615$ showed the highest efficiency for all cases because heat transfer augmentations at $Re = 615$ were near those at $Re = 1016$, while the friction factor augmentations were several percent lower. Generally speaking, friction factor augmentations dictated the efficiency results, because there was a wider range in friction factor augmentations than in heat transfer augmentations.

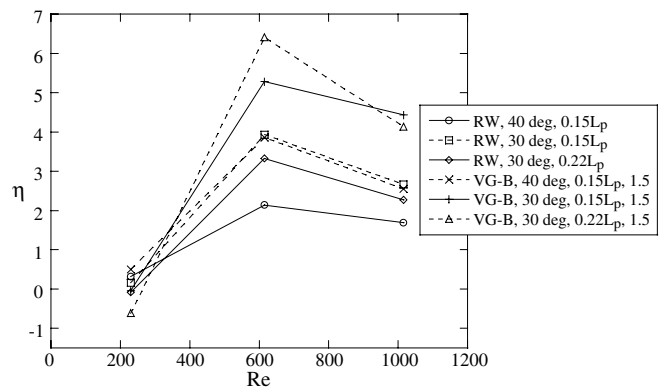


Fig. 15. Efficiency index comparisons for winglet shape, α , and Z at all Re .

The best overall performer based on efficiency index was VG-B winglets at $\alpha = 30^\circ$ and $Z = 0.22L_p$. This case produced 6.5 and 4.5 times as much heat transfer augmentation as friction factor augmentation at $Re = 615$ and 1016, respectively.

9. Conclusions

Augmenting the heat transfer along the tube wall of a compact heat exchanger can lead to lighter weight heat exchangers that require less space than current exchanger designs. To this end, an experimental investigation was presented whereby winglets placed on the louvers of a louvered fin compact heat exchanger were evaluated in terms of increased heat transfer augmentations, friction factor augmentation, and efficiency index. Several winglet parameters were investigated including the following: angle of attack, distance of the winglet from the tube wall, aspect ratio, Reynolds number, winglet direction, winglet orientation, and winglet shape. Using a design of experiments, general trends for many of these parameters were found. Further testing of the remaining parameters not included in the design of experiments test matrix produced detailed direct comparisons of the important parameters.

Regarding Reynolds number, at the lowest Reynolds number tested ($Re = 230$), none of the winglet setups produced augmentations greater than 4%. Augmentations at Reynolds numbers of 615 and 1016 were much higher than those at 230, resulting from the higher velocities reacting more to the blockage caused by the winglets. Friction factor augmentation also increased with Reynolds number.

In general, heat transfer augmentation increased with increasing angle of attack, increasing winglet size (decreasing aspect ratio in this case), and with decreasing winglet distance from the wall. For an angle of attack of 20° , the results showed little augmentation; however, angles of attack greater than or equal to 30° performed very well. An aspect ratio of 3 did not provide much benefit while an aspect ratio of 1.5 produced high augmentations. Doubling the surface area of a winglet to make rectangular winglets increased the heat transfer augmentation. The best heat transfer augmentation was found with rectangular

winglets giving 38%, 36%, and 3% at Reynolds numbers of 1016, 615, and 230, respectively.

There were three primary winglet orientations and directions tested: winglets all aimed towards the wall, alternating winglet direction and orientation, and alternating winglet direction with backward winglets throughout. In the configuration where all of the winglets were aimed towards the wall in the VG-F configuration, the average heat transfer augmentations were typically very low. When the winglet direction and orientation were alternated on every other louver, results were significantly improved with a maximum augmentation of 25%. When all winglets were placed in the VG-B orientation with alternating direction, results improved yielding augmentations of up to 33%.

As mentioned earlier, parameter levels that yielded higher heat transfer augmentations also produced higher friction factor augmentations. Decreasing the winglet size and angle of attack decreased the friction factor augmentations while no strong generalizations could be made about winglet distance from wall. The best performers for the efficiency index also had the lowest friction factor augmentations.

It has been shown through several experiments that tube wall heat transfer augmentations with a relatively small pressure drop penalties can be achieved through the use of winglets placed on the louvers of a compact heat exchanger. As winglets could be produced by the same stamping process used to shape the louvers, this is not a purely academic exercise, but a viable method to be incorporated into actual production louvered fin exchangers.

Acknowledgements

The authors would like to acknowledge the support of Modine Manufacturing, Inc for their support on this project. In particular the authors would like to thank Drs. Victor Nino and Steve Memory who have provided technical feedback for this work.

References

- [1] W.M. Kays, A.L. London, *Compact Heat Exchangers*, second ed., McGraw-Hill, New York, 1984.

- [2] A. Achaicha, T.A. Cowell, Heat transfer and pressure drop characteristics of flat tube and louvered plate fin surfaces, *Exp. Therm. Fluid Sci.* 1 (1988) 147–157.
- [3] R.L. Webb, P. Trauger, Flow structures in louvered fin heat exchanger geometry, *Exp. Therm. Fluid Sci.* 4 (1991) 205–214.
- [4] K.N. Atkinson, R. Draulic, M.R. Heikal, T.A. Cowell, Two- and three-dimensional numerical models of flow and heat transfer over louvered fin arrays in compact heat exchangers, *Int. J. Heat Mass Transfer* 41 (1998) 4063–4080.
- [5] J. Cui, D.K. Tafti, Computations of flow and heat transfer in a three-dimensional multilouvered array fin geometry, *Int. J. Heat Mass Transfer* 45 (2002) 5007–5023.
- [6] D.K. Tafti, J. Cui, Fin-tube junction effects on flow and heat transfer in flat tube multilouvered heat exchangers, *Int. J. Heat Mass Transfer* 46 (2003) 2027–2038.
- [7] P. Ebeling, K.A. Thole, Measurements and predictions of the heat transfer at the tube-fin junction for louvered fin heat exchangers, *Int. J. Compact Heat Exchang.* 5 (2004) 265–286.
- [8] M.C. Gentry, A.M. Jacobi, Heat transfer enhancement by delta-wing-generated tip vortices in flat plate and developing channel flows, *J. Heat Transfer* 124 (2002) 1158–1168.
- [9] Y. Chen, M. Fiebig, N.K. Mitra, Heat transfer enhancement of a finned oval tube with punched longitudinal vortex generators in-line, *Int. J. Heat Mass Transfer* 41 (1998) 4151–4166.
- [10] S. Tiwari, D. Maurya, G. Biswas, V. Eswaran, Heat transfer enhancement in cross-flow heat exchangers using oval tubes and multiple delta winglets, *Int. J. Heat Mass Transfer* 46 (2003) 2841–2856.
- [11] A. Joardar, A.M. Jacobi, Impact of leading edge delta-wing vortex generators on the thermal performance of a flat tube, louvered-fin compact heat exchanger, *Int. J. Heat Mass Transfer* 48 (2005) 1480–1493.
- [12] A.C. Lyman, R.A. Stephan, K.A. Thole, L. Zhang, S. Memory, Scaling of heat transfer coefficients along louvered fins, *Exp. Therm. Fluid Sci.* 26 (2002) 547–563.
- [13] R.A. Stephan, K.A. Thole, Optimization study relevant to louvered fin heat exchangers, *Int. J. Heat Exchang.* 6 (2005) 73–92.
- [14] M.E. Springer, K.A. Thole, Experimental design for flowfield studies of louvered fins, *Exp. Therm. Fluid Sci.* 18 (1998) 258–269.
- [15] M.F. Modest, *Radiative Heat Transfer*, second ed., Academic Press, New York, 2003.
- [16] F.M. White, *Fluid Mechanics*, fourth ed., McGraw-Hill, New York, 1999.
- [17] R.J. Moffat, Describing the uncertainties in experimental results, *Exp. Therm. Fluid Sci.* 1 (1988) 3–17.
- [18] R.K. Roy, *Design of Experiments Using the Taguchi Approach: 16 Steps to Product and Process Improvement*, John Wiley & Sons, New York, 2001.